

• Original Paper •

Seesaw Pattern of Rainfall Anomalies between the Tropical Western North Pacific and Central Southern China during Late Summer

Xinyu LI^{1,2,3} and Riyu LU^{*1,2}

¹State Key Laboratory of Numerical Modeling for Atmospheric Sciences and Geophysical Fluid Dynamics,
Institute of Atmospheric Physics, Chinese Academy of Sciences, Beijing 100029, China

²College of Earth and Planetary Sciences, University of the Chinese Academy of Sciences, Beijing 100049, China

³College of Oceanography, Hohai University, Nanjing 210098, China

(Received 15 June 2018; revised 3 September 2018; accepted 12 October 2018)

ABSTRACT

It is well known that suppressed convection in the tropical western North Pacific (WNP) induces an anticyclonic anomaly, and this anticyclonic anomaly results in more rainfall along the East Asian rain band through more water vapor transport during summer, as well as early and middle summer. However, the present results indicate that during late summer (from mid-August to the beginning of September), the anomalous anticyclone leads to more rainfall over central southern China (CSC), a region quite different from preceding periods. The uniqueness of late summer is found to be related to the dramatic change in climatological monsoon flows: southerlies over southern China during early and middle summer but easterlies during late summer. Therefore, the anomalous anticyclone, which shows a southerly anomaly over southern China, enhances monsoonal southerlies and induces more rainfall along the rain band during early and middle summer. During late summer, however, the anomalous anticyclone reflects a complicated change in monsoon flows: it changes the path, rather than the intensity, of monsoon flows. Specifically, during late summers of suppressed convection in the tropical WNP, southerlies dominate from the South China Sea to southern China, and during late summers of enhanced convection, northeasterlies dominate from the East China Sea to southern China, causing more and less rainfall in CSC, respectively.

Key words: tropical western North Pacific, monsoon flows, precipitation, late summer

Citation: Li, X. Y., and R. Y. Lu, 2019: Seesaw pattern of rainfall anomalies between the tropical western North Pacific and central southern China during late summer. *Adv. Atmos. Sci.*, **36**(3), 261–270, <https://doi.org/10.1007/s00376-018-8130-6>.

1. Introduction

The summer rainfall over eastern China is significantly affected by the anomalous convective activity over the tropical western North Pacific (WNP) (e.g., Nitta, 1987; Lu, 2001a,b, 2004; Kosaka et al., 2011; Li and Lu, 2017). Anomalous convection (or precipitation) over the tropical WNP induces an anticyclonic/cyclonic anomaly in the lower troposphere to the northwest, as a result of a Gill response (Lu, 2001a). An anticyclonic/cyclonic anomaly corresponds to the westward extension/eastward retreat of the WNP subtropical high and favors enhanced/suppressed rainfall along the climatological East Asian rain band by modifying water vapor transport (e.g., Kurihara and Tsuyuki, 1987; Huang and Sun, 1992; Lu and Dong, 2001; Zhou and Yu, 2005; Kosaka et al., 2011; Hu et al., 2017). Therefore, the subtropical WNP anticyclonic/cyclonic anomaly plays a crucial role in inducing the well-known seesaw pattern of rainfall anomalies

over the tropical WNP and East Asian rain band. In addition, the subtropical WNP anticyclonic anomaly, which often appears during El Niño decaying summers, also plays an important role in linking East Asian summer climate anomalies to ENSO (Wang et al., 2000; Lin and Lu, 2009; Chen et al., 2012, 2016; Li et al., 2014).

It is well known that both the rain band and large-scale circulation in the WNP and East Asia exhibits remarkable seasonal evolution during summer (e.g., Tao and Chen, 1987; Qian and Lee, 2000; Wu and Wang, 2001; Chen et al., 2004; Ding and Chan, 2005; Zhao et al., 2007; Lin and Lu, 2008; Su and Xue, 2010; Chu et al., 2012; Oh and Ha, 2015). In mid-May, the WNP subtropical high advances northeastward and the monsoon trough establishes over the eastern South China Sea. Consequently, the monsoon rain band appears over South China. In mid-June, the WNP subtropical high advances northward and the monsoon trough migrates northeastward. Correspondingly, the monsoon rain band advances northward into the Yangtze River basin. In late July, the WNP subtropical high marches further northward and retreats eastward and the monsoon trough also extends further

* Corresponding author: Riyu LU
Email: lr@mail.iap.ac.cn

northeastward. Coinciding with this northward shift of the subtropical high, the monsoon rain band advances northward to North China. Overall, the evolution of monsoon rainfall corresponds well to the evolution of large-scale circulation.

Associated with the subseasonal evolution of the basic flow, the subtropical WNP anticyclonic/cyclonic anomaly extends gradually northward from early to late summer (Ye and Lu, 2011; Hu et al., 2017). Concurrently, the positive/negative rainfall anomalies in eastern China advances from South China to Huai River basin. The northward extension of the subtropical WNP anticyclonic/cyclonic anomaly is due to the change in the basic flow, i.e., the northward jump of the East Asian westerly jet in the upper troposphere and the northward advance of the WNP subtropical high in the lower troposphere (Kosaka and Nakamura, 2010; Ye and Lu, 2011; Hu et al., 2017; Li and Lu, 2018). Recently, Li and Lu (2018) investigated the subseasonal change in the seesaw relationship in precipitation between the tropical WNP and the Yangtze River basin, and found that this relationship experiences considerable subseasonal changes from early to mid-summer. The rainfall anomalies over eastern China associated with the anomalous tropical WNP precipitation appear over the Yangtze River basin during early summer, but advance northward to the Huanghe-Huaihe River during mid-summer, which is attributable to the northward extension of the subtropical WNP anticyclonic/cyclonic anomaly.

In previous results, there is a good correspondence between the circulation and rainfall anomalies; or more specifically, the rainfall anomalies always appear at the north flank of the subtropical WNP anticyclonic/cyclonic anomaly. However, in this study, we show an exception: during late summer the rainfall anomalies appear at the west flank of the subtropical WNP anticyclonic/cyclonic anomaly. The aim of this study is to investigate this unique feature of late summer and the physical mechanism responsible for this change in the relationship between circulation and rainfall anomalies.

The rest of the paper is arranged as follows: Section 2 describes the data and methods used in this study. Section 3 shows the anomalies of rainfall and circulation associated with the tropical WNP precipitation during late summer. To illustrate the uniqueness of late summer, we also show some results during mid-summer and make a comparison between these two periods. In section 4, we investigate the possible mechanism responsible for the unique feature of late summer, by examining circulation and rainfall, rather than their anomalies, which have been widely used to study the circulation–rainfall relationship. Section 5 is a summary of our findings.

2. Data and methods

The data used in this study include: (1) daily data from the Japanese 55-year Reanalysis (Kobayashi et al., 2015); (2) pentad precipitation data from NOAA's Climate Prediction Center Merged Analysis of Precipitation (CMAP; Xie and Arkin, 1997); and (3) daily rainfall data at stations in the China Daily Ground Climate Dataset (Version 3.0), pro-

vided by the National Meteorological Information Center of the China Meteorological Administration. There are a total of 824 stations in this dataset. The present study uses these daily rainfall data at stations screened by Han et al. (2014), who retained 679 stations after excluding those stations with a large amount of missing data. The period of coverage for all the data is 1 June to 30 September 1979–2014.

The tropical WNP precipitation index (WNPPI) is defined as the precipitation anomalies averaged over the region (10° – 20° N, 115° – 150° E) and then multiplied by minus one. The region used to define the WNPPI is identical to that used in our previous study (Li and Lu, 2018). As mentioned in the introduction, the interannual variability in precipitation over this region is closely associated with the subtropical WNP anticyclonic/cyclonic anomaly in the lower troposphere. The sign change in the index exhibits the subtropical WNP anticyclonic anomaly that favors enhanced rainfall over eastern China.

In this study, the Student's *t*-test is used to determine the statistical significance. As precipitation exhibits larger interannual variability than circulation, we use the 90% confidence level for precipitation anomalies and the 95% confidence level for circulation anomalies.

3. Rainfall and circulation anomalies associated with the WNPPI during mid- and late summer

Figure 1 shows the rainfall anomalies over stations regressed onto the normalized WNPPI during pentads 39–45 (mid-summer) and pentad 46–49. Here, mid-summer is defined as the period from pentad 39 to pentad 45, i.e., from 10 July to 13 August, following Li and Lu (2018). The precipitation anomalies during pentad 46–49 exhibit some appreciable differences with those during mid-summer. First, significant positive anomalies for mid-summer mainly appear over the Huanghe-Huaihe River (Fig. 1a), consistent with our previous study (Li and Lu, 2018). By contrast, the positive anomalies for pentad 46–49 mainly appear over the central southern China (hereafter denoted as CSC, and shown by the red polygons in Fig. 1b), basically including Guangxi, Hunan and Hubei provinces (Fig. 1b). Over CSC, 59 out of the 94 stations show significant positive correlation (at the 90% confidence level) with the WNPPI for pentads 46–49. It is also notable that the defined CSC region here includes the middle reaches of the Yangtze River basin, as defined by Li and Lu (2018), which is consistent with the strong correlation coefficients in precipitation between the tropical WNP and the Yangtze River basin after mid-summer shown in their Fig. 2a. Second, there are significant negative anomalies over South China during mid-summer (Fig. 1a), while negative anomalies during pentads 46–49 only appear over a small region along the southeast coast of the mainland China (Fig. 1b). Third, the negative anomalies for pentads 46–49 are stronger compared to those during mid-summer. These differences suggest that the spatial pattern of rainfall anomalies over eastern China associated with the tropical WNP precipitation ex-

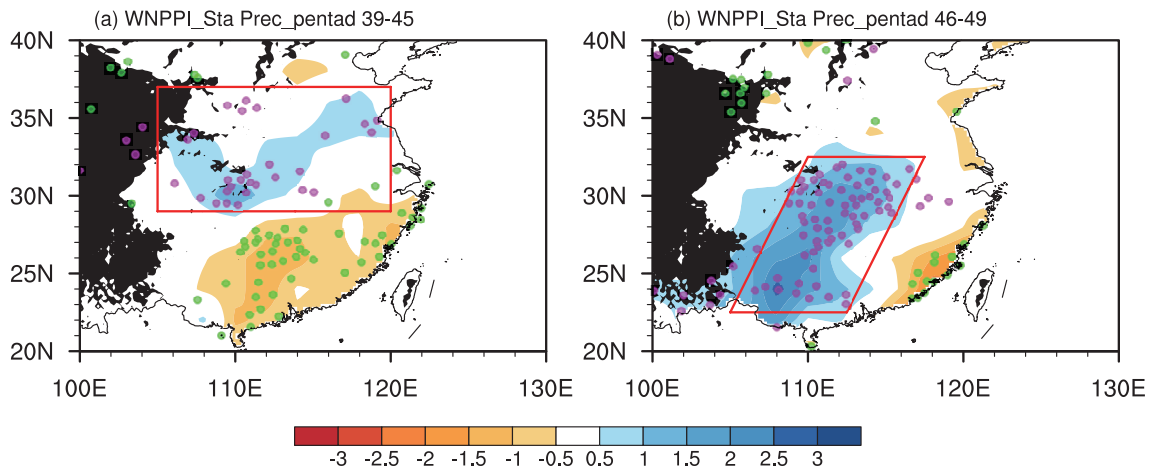


Fig. 1. Regression of rainfall anomalies (units: mm d^{-1}) with respect to the normalized WNPPI during (a) pentads 39–45 (mid-summer) and (b) pentads 46–49. The magenta and green dots represent the stations with positive and negative anomalies significant at the 90% confidence level, based on the Student’s *t*-test, respectively. The polygons in (a) and (b) represent the regions of the Huanghe-Huaihe River and CSC, respectively.

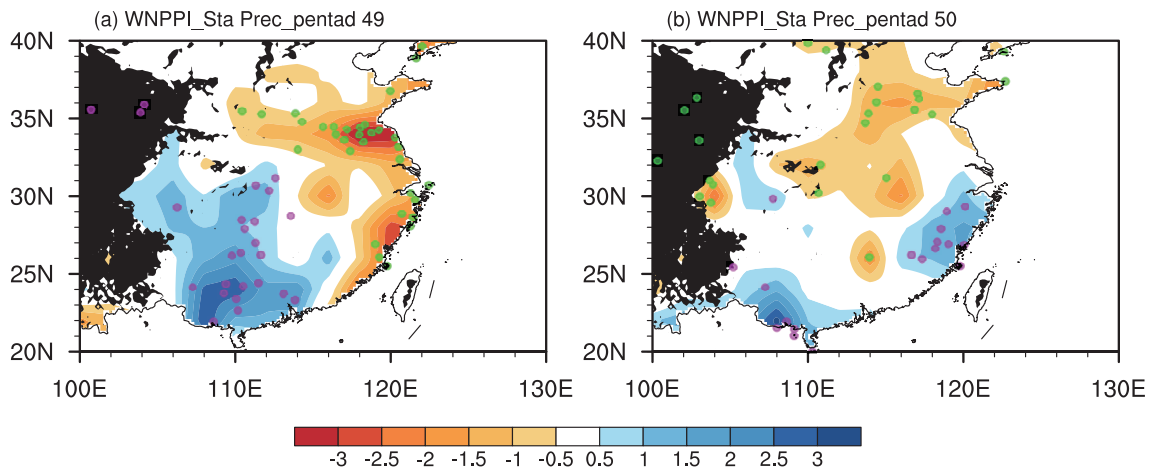


Fig. 2. Regression of rainfall anomalies (units: mm d^{-1}) with respect to the normalized WNPPI during (a) pentad 49 and (b) pentad 50. The magenta and green dots represent the stations with positive and negative anomalies significant at the 90% confidence level, based on the Student’s *t*-test, respectively.

perience a subseasonal change at the end of mid-summer.

Figure 2 shows the rainfall anomalies over stations regressed onto the normalized WNPPI during pentad 49 and pentad 50, to show that pentads 46–49 can be precisely considered as the period for this spatial pattern. There are positive anomalies over CSC during pentad 49 (Fig. 2a). However, the rainfall anomalies over CSC are very weak for pentad 50 (Fig. 2b). The correlation coefficients between the WNPPI and the rainfall averaged over CSC during pentad 49 is 0.36, significant at 95% confidence level, but that for pentad 50 is only 0.01. We have also examined the WNPPI-associated rainfall anomalies for each pentad from pentad 51 to 55, and found they are very weak in CSC (not shown). Therefore, in the following, we define the period from pentad 46 to pentad 49, i.e., from 14 August to 2 September, as late summer. The definitions for both mid-summer and late summer are based on the change in the anomalous rainfall pattern over eastern China associated with the WNPPI, which mainly

appear over the Huanghe-Huaihe River during mid-summer and over CSC during late summer.

Figure 3 shows the normalized time series of precipitation

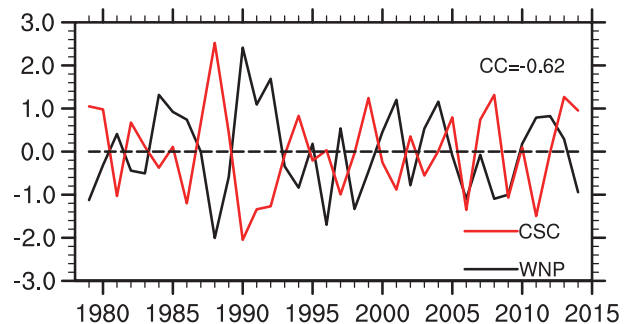


Fig. 3. Normalized time series of the rainfall anomalies averaged over CSC (red line) and the tropical WNP (black line) during late summer. Units: mm d^{-1} .

averaged over the tropical WNP and the stations in CSC for late summer. The rainfall over these two regions exhibits a clear out-of-phase relationship, with a correlation coefficient of -0.62 , which is significant at the 99% confidence level. On the other hand, both series show clear interannual variations and no distinct decadal variations. The decadal components of both series only accounts for 3%–4% of the total variance if we define the decadal variation as the 9-yr running mean, suggesting the decadal variability is much weaker than the interannual variability.

Figure 4 shows the 850-hPa wind and precipitation anomalies regressed onto the normalized WNPPI during mid-summer and late summer. The bottom panels highlight the anomalies over eastern China. For both mid-summer and late summer, similar negative precipitation anomalies appear over the tropical WNP, and induce an anticyclonic anomaly over the subtropical WNP (Figs. 4a and b). The spatial pattern of the anticyclonic anomaly during late summer is almost

same as that during mid-summer, especially that over eastern China, where the wind anomalies are characterized by similar southwesterlies. We project the wind anomalies onto the northeast direction across CSC from $(22.5^{\circ}\text{N}, 105^{\circ}\text{E})$ to $(32.5^{\circ}\text{N}, 115^{\circ}\text{E})$, as indicated by the red dashed lines in Figs. 4c and d. The projected wind anomalies averaged along this trace is 1.48 m s^{-1} for late summer, very close to that for mid-summer (1.36 m s^{-1}). However, the spatial pattern of rainfall anomalies over eastern China, which corresponds well to the convergence anomalies of water vapor flux, shows distinctly different features between mid-summer and late summer, as shown in Fig. 1. For mid-summer (Fig. 4c), positive rainfall anomalies appear over the north flank of the subtropical WNP anticyclonic anomaly and negative rainfall anomalies appear over South China. For late summer (Fig. 4d), on the other hand, positive rainfall anomalies under similar circulation anomalies mainly appear over CSC. The rainfall anomaly averaged over CSC during late summer is 1.18 mm d^{-1} , while

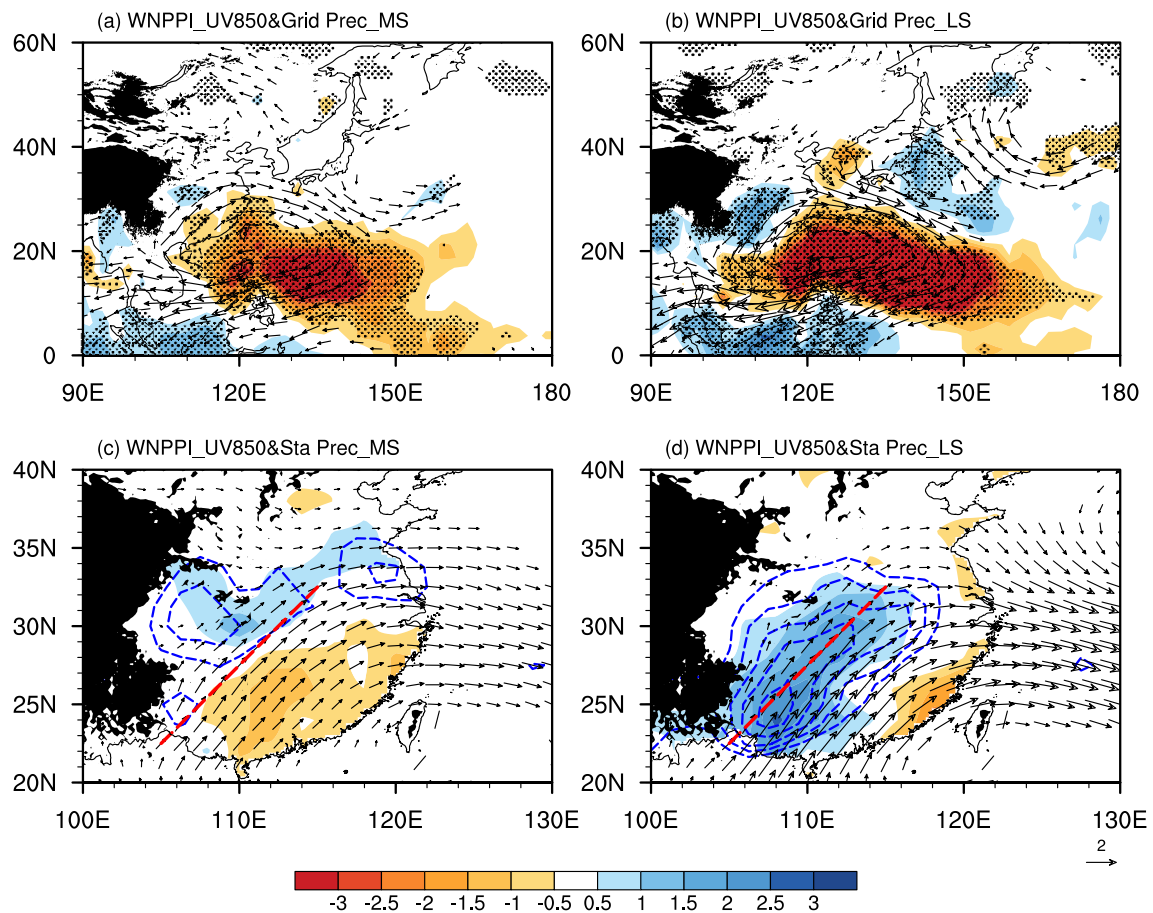


Fig. 4. Regression of the 850-hPa horizontal winds (vectors; units: m s^{-1}) and precipitation (shading; units: mm d^{-1}) with respect to the normalized WNPPI during (a, c) mid-summer and (b, d) late summer. The rainfall anomalies in (a) and (b) are based on the CMAP data and the black dots denote the 90% confidence level for precipitation anomalies, based on the Student's t -test. Panels (c, d) are a zoomed-in view of the anomalies over eastern China, which are based on the station rainfall data. Blue contours show the convergence anomalies of the water vapor flux, which is integrated from the surface to 100 hPa, with respect to the normalized WNPPI (contour interval: $0.5 \times 10^{-5} \text{ kg m}^{-2} \text{ s}^{-1}$). Only the vectors of either zonal or meridional wind anomalies significant at the 95% confidence level are shown. Red dashed lines from $(22.5^{\circ}\text{N}, 105^{\circ}\text{E})$ to $(32.5^{\circ}\text{N}, 115^{\circ}\text{E})$ indicate the trace used for analyzing the southwesterly anomalies. The black shading represents mountains higher than 1500 m.

it is only -0.07 mm d^{-1} for mid-summer. These results suggest that the significant rainfall anomalies over CSC during late summer cannot be visually explained by the circulation anomalies.

The results in this section indicate that the similar large-scale circulation anomalies between mid-summer and late summer correspond to very different precipitation anomalies. This puzzle is investigated in the next section.

4. Circulation–rainfall correspondence in original fields and climatology

4.1. Original fields

The preceding section presents a puzzle: the relationship between circulation and rainfall anomalies is different between mid-summer and late summer, which is quite different from the well-known fact that the subtropical WNP anti-cyclonic/cyclonic anomaly greatly affects rainfall anomalies in eastern China during summer or the mei-yu season. The circulation–rainfall relationship shown in the preceding section is from the perspective of anomalies, i.e., the relationship between the anomalies of circulation and rainfall. However, the circulation–rainfall relationship is in nature established by the original fields, i.e., a certain pattern of circulation induces its corresponding pattern of rainfall (Su et al., 2014). Therefore, we investigate the correspondence between rainfall and circulation from the perspective of original values in this section.

We choose the years in which the absolute values of the WNPPI are greater than 0.7 standard deviations during late summer and perform composite analyses based on these years. This criterion yields 10 positive years (1979, 1988, 1994, 1996, 1998, 2002, 2006, 2008, 2009, and 2014) and 10 negative years (1984, 1985, 1986, 1990, 1991, 1992, 2001,

2004, 2011, and 2012). We also used some other criteria, such as 0.8 or 1.0 standard deviations, and obtained similar results (not shown).

Figure 5 shows the composite 850-hPa wind and rainfall for the positive and negative WNPPI cases during late summer. For the positive WNPPI cases (Fig. 5a), the monsoon flows are characterized by southerlies from the ocean to mainland China and results in rainfall there, including CSC. The southerlies are associated with the westerlies in the tropics, which turn into southerlies in the South China Sea with a cyclonic-like circulation. For the negative cases (Fig. 5b), on the other hand, the monsoon flows feature a cyclone over the tropical WNP, and associated with this cyclone are the strong northeasterlies over CSC. As a result, the rainfall is very weak over CSC, but it mainly appears along the southeast coast of mainland China where the high humidity is (not shown). Overall, the original circulation for positive and negative WNPPI cases matches well with the rainfall over CSC.

Figure 6 shows the water vapor flux integrated from the surface to 100 hPa and the rainfall over grids for the positive and negative WNPPI cases during late summer. The water vapor flux for both the positive and negative cases resembles the corresponding circulation at 850 hPa (Fig. 5), suggesting the lower-tropospheric circulation plays a crucial role in water vapor transport. For the positive WNPPI cases, the zonal water vapor transport over the tropical WNP is weak, resulting in weak rainfall there. Instead, there is water vapor transport from the South China Sea to mainland China, including CSC. For the negative cases, on the other hand, there is strong water vapor transport by the westerlies to the tropical WNP, resulting in strong precipitation there. The enhanced precipitation over the tropical WNP induces a cyclonic anomaly, which favors the appearance of the cyclone over the tropical WNP and the resultant weak rainfall over CSC (Fig. 5b).

These results suggest that the circulation corresponds

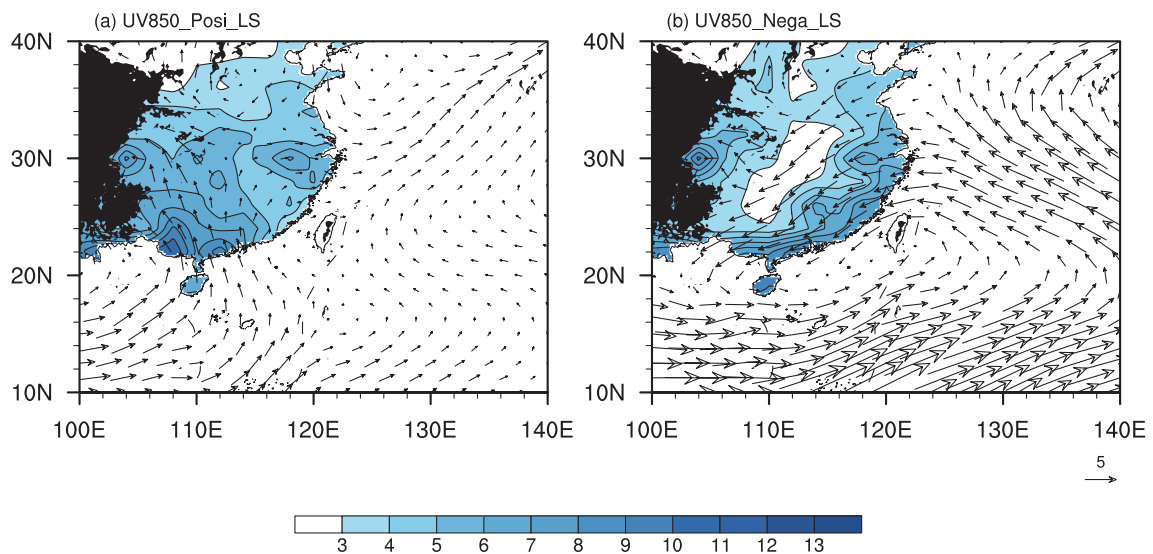


Fig. 5. Composite 850-hPa horizontal wind (vectors; units: m s^{-1}) and rainfall over stations in China (shading and contours; units: mm d^{-1}) for (a) positive and (b) negative WNPPI cases during late summer.

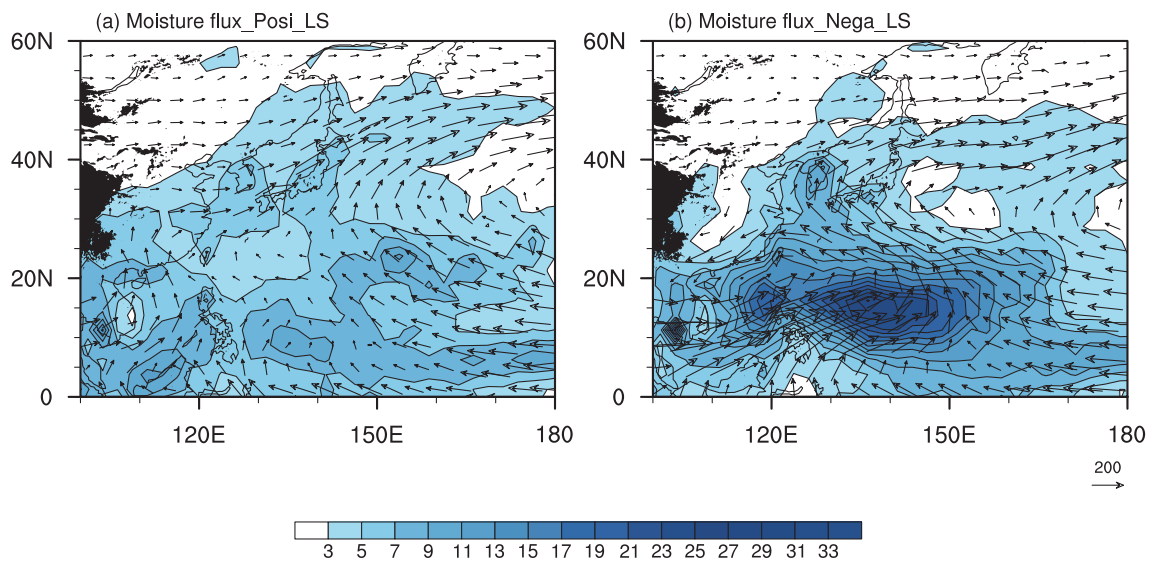


Fig. 6. Composite water vapor flux integrated from the surface to 100 hPa (vectors; units: $\text{kg m}^{-1} \text{s}^{-1}$) and rainfall over grids (shading and contours; units: mm d^{-1}) for (a) positive and (b) negative WNPPI cases during late summer.

well to the rainfall over CSC from the viewpoint of the original fields, which is consistent with the fact that the summer rainfall over eastern China is affected by the monsoonal circulation. On the other hand, the correspondence of circulation and rainfall still seems to be a puzzle from the viewpoint of the anomalies, and this issue is further investigated in the following section.

4.2. Climatology

The present results suggest the circulation–rainfall relationship during late summer is well established from the viewpoint of the original fields, while this seems not to be the case for the anomalies, as shown in section 3. The original field is a combination of anomalies and the climatological mean, and therefore it can be inferred that the climatological state may play a crucial role in the unique spatial pattern of rainfall during late summer. In the following, we investigate the climatology of circulation and rainfall to test this hypothesis.

Figure 7 shows the climatology of 850-hPa horizontal wind and rainfall over eastern China during mid-summer and late summer. The circulation and the corresponding rainfall during late summer exhibit distinctly different features from those during mid-summer. For mid-summer (Fig. 7a), the monsoonal circulation is characterized by southerlies and southwesterlies that transport water vapor from the ocean to eastern China and result in rainfall there. There are two maximum rainfall centers associated with the southerlies and southwesterlies: one is located over the south coast of mainland China and the other appears over the Yangtze River basin and the Huanghe-Huaihe River basin, where the rainfall is basically greater than 5.0 mm d^{-1} . However, during late summer (Fig. 7b), the monsoon flows exhibit distinctly different features. The monsoon trough extends eastward and the monsoon flows are mainly characterized by the easterlies along

the south coast of mainland China and weak northeasterlies over CSC. As a result, substantial rainfall appear over the southeast coast of mainland China, while the rainfall over CSC is very weak.

Some values can be used to further illustrate the different impacts of the similar subtropical WNP anticyclonic anomaly on the monsoon flows during mid-summer and late summer. For mid-summer, the meridional wind averaged along (23.75°N , $107.5^\circ\text{--}117.5^\circ\text{E}$), which can be used to represent the entrance of water vapor transport to Southeast China and is shown by the horizontal red dashed lines, is 3.70 m s^{-1} for the positive WNPPI cases and 1.59 m s^{-1} for the negative cases. The positive and negative WNPPI cases here are also chosen based on the ± 0.7 standard deviations of the WNPPI. These values exhibit the same sign as the climatological mean (2.78 m s^{-1}). However, for late summer, the meridional wind averaged along this trace are 1.59 m s^{-1} and -2.02 m s^{-1} for the positive and negative WNPPI cases, respectively, and that for the climatological mean is near to zero (0.37 m s^{-1}). These values confirm that the subtropical WNP anticyclonic anomaly can change the path of the monsoon flows during late summer, but only change the strength of the southerlies during mid-summer.

The equivalent potential temperature (θ_e) has been widely used to describe the East Asian summer monsoon, since the monsoon flows are characterized by warm and humid air (Ding, 2005). A higher θ_e indicates a more humid and warmer weather condition. Figure 8 shows the climatology of θ_e for mid-summer and late summer, and 850-hPa horizontal wind is also given to facilitate comparison. The θ_e shows distinct different features between mid-summer and late summer. For mid-summer (Fig. 8a), the high θ_e values dominant the region south of the Yangtze River, including CSC, in a tongue-shaped pattern. The high θ_e values are associated with the monsoonal southerlies (Fig. 7a), which result in a warm and

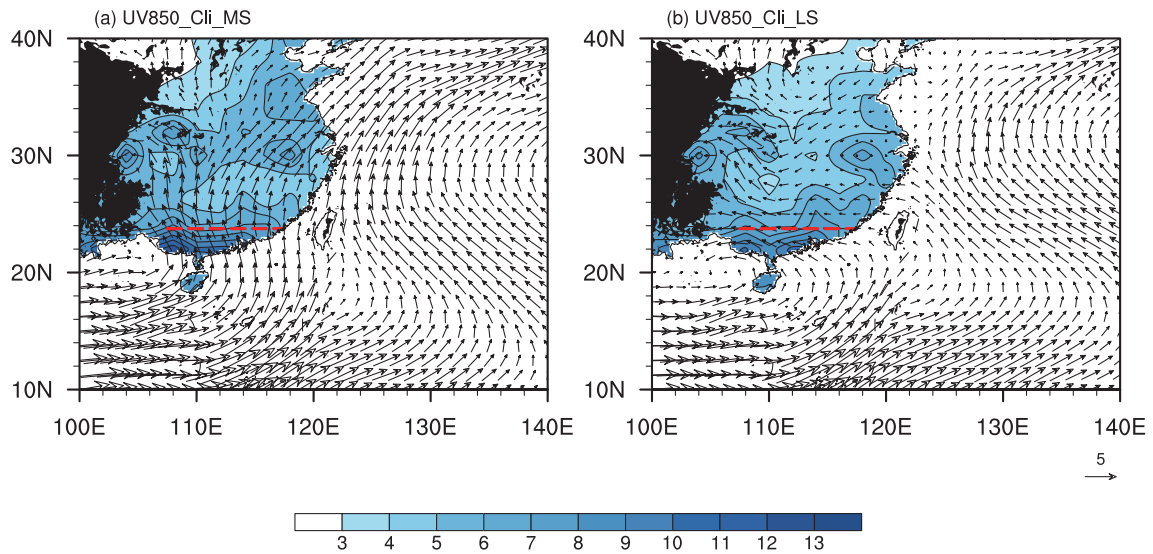


Fig. 7. Climatology of the 850-hPa wind (vectors; units: m s^{-1}) and rainfall (shading; units: mm d^{-1}) during (a) mid-summer and (b) late summer. Red dashed lines along $(23.75^\circ\text{N}, 107.5^\circ\text{E}–117.5^\circ\text{E})$ denote the trace used for later analysis.

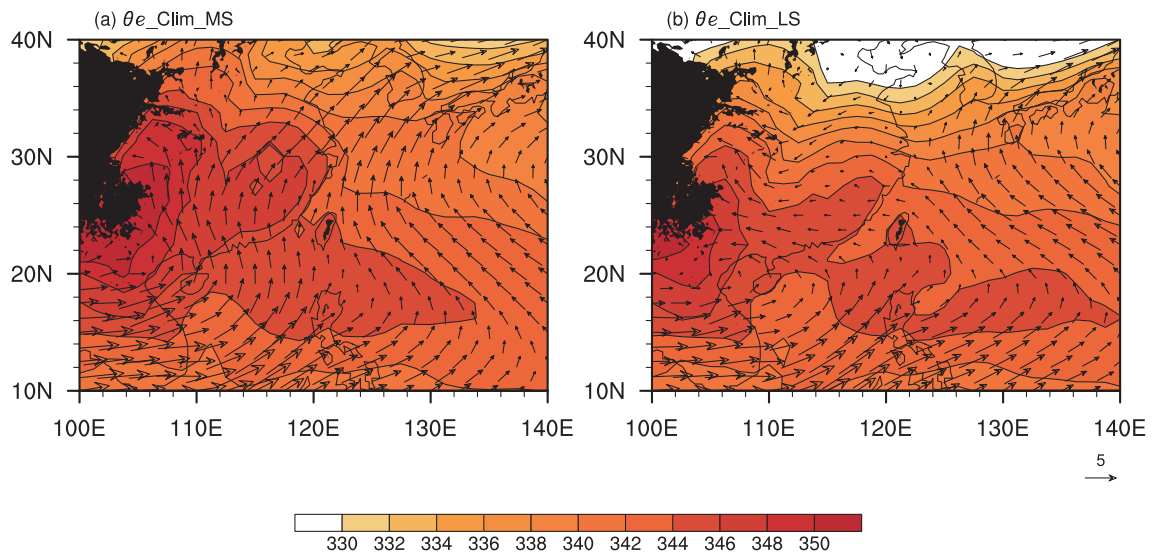


Fig. 8. Climatology of the θ_e (shading; units: K) and 850-hPa wind (vectors; units: m s^{-1}) during (a) mid-summer and (b) late summer.

highly humid condition. For late summer (Fig. 8b), on the other hand, the high θ_e values only appear along the southeast coast of mainland China, which is associated with the easterlies of the monsoon flows (Fig. 7b). However, the θ_e over CSC is weak, which is associated with the northeasterlies. The distinct monsoon flows indeed result in different thermal conditions over eastern China between mid-summer and late summer.

Figure 9 shows the climatological evolution of the zonal and meridional winds averaged along $(23.75^\circ\text{N}, 107.5^\circ\text{E}–117.5^\circ\text{E})$. The evolution of both zonal and meridional winds corresponds well with the defined periods of mid-summer and late summer. During mid-summer, the southerlies dom-

inate but gradually transfer into southeasterlies. At the end of mid-summer, the meridional wind is near to zero, and the easterlies dominate during late summer. The meridional wind is 2.78 m s^{-1} for mid-summer and becomes close to zero (0.37 m s^{-1}) during late summer.

Figure 10 shows the climatological evolution of the southwesterlies averaged along the trace from $(22.5^\circ\text{N}, 105^\circ\text{E})$ to $(32.5^\circ\text{N}, 115^\circ\text{E})$ at 850 hPa. It can be clearly observed that the evolution of the southwesterlies also corresponds well with the transition of mid-summer to late summer. There are southwesterlies during mid-summer, and the southwesterlies translate into northeasterlies during late summer, which is consistent with the results shown in Fig. 7. The

southwesterlies are 1.88 m s^{-1} averaged over mid-summer, but -1.20 m s^{-1} during late summer.

In summary, both Figs. 9 and 10 indicate that the monsoon flows exhibit a drastic change exactly at the end of mid-summer and the beginning of late summer. This is interesting, because the periods of mid-summer and late summer are defined according to the change in the relationship of precipitation anomalies between the tropical WNP and eastern China. However, this consistency between the changes in the relationship and in the monsoon flows is not by coincidence, and

reconfirms that the climatological monsoon flows play a crucial role in affecting the relationship of precipitation between the tropical WNP and eastern China.

5. Conclusions

It is well known that suppressed precipitation over the tropical WNP induces an anticyclonic anomaly over the subtropical WNP, and this anticyclonic anomaly favors enhanced rainfall along the East Asian rain band by enhancing water vapor transport during summer. This seesaw pattern of rainfall anomalies also exists on subseasonal time scales, including early summer and mid-summer (Li and Lu, 2018). However, this study shows a distinctly different rainfall pattern during late summer (14 August to 2 September): the suppressed precipitation over the tropical WNP also induces the subtropical WNP anticyclonic anomaly, but results in more rainfall over CSC, a region roughly covering Guangxi, Hunan and Hubei provinces.

This unique pattern of rainfall anomalies in late summer is found to be related to the special climatological monsoon flows, which experience a dramatic change from the earlier period to late summer. Climatologically, during early summer and mid-summer, the monsoon flows are mainly characterized by the southerlies over southern China. However, during late summer, the monsoon trough extends eastward and the monsoon flows feature the easterlies over southern China. Therefore, the subtropical WNP anticyclonic anomaly, which accompanies anomalous southerlies over southern China, enhances the monsoonal southerlies and results in more rainfall along the rain band during early summer and mid-summer. For late summer, however, the anomalous anticyclone does not simply overlap with the climatological monsoon flows, and thus reflects a complicated change in monsoon flows, rather than the simple increase in monsoon flows as in early summer and mid-summer. In other words, the anticyclonic/cyclonic anomaly could result in the change in the path of monsoon flows during late summer: the southerlies associated with the anticyclonic anomaly combine with the climatological easterlies and result in southerlies or southeasterlies from southern China to CSC, causing more rainfall there. By contrast, the northerlies associated with the cyclonic anomaly combine with the climatological easterlies and result in northeasterlies from the East China Sea to southern China, causing less rainfall in CSC. This study suggests that the climatological monsoon flows should be taken into consideration, when circulation anomalies are used to explain precipitation anomalies.

Subseasonal changes in the rainfall pattern may result from the subseasonal change of the monsoon flow, or from the subseasonal change of the circulation anomalies associated with the WNPPI. This study indicates that the spatial patterns of WNP circulation anomalies are similar during mid-summer and late summer, and thus highlights the role of monsoon flow change. This is different from our previous study, which highlighted the difference in circulation anomalies dur-

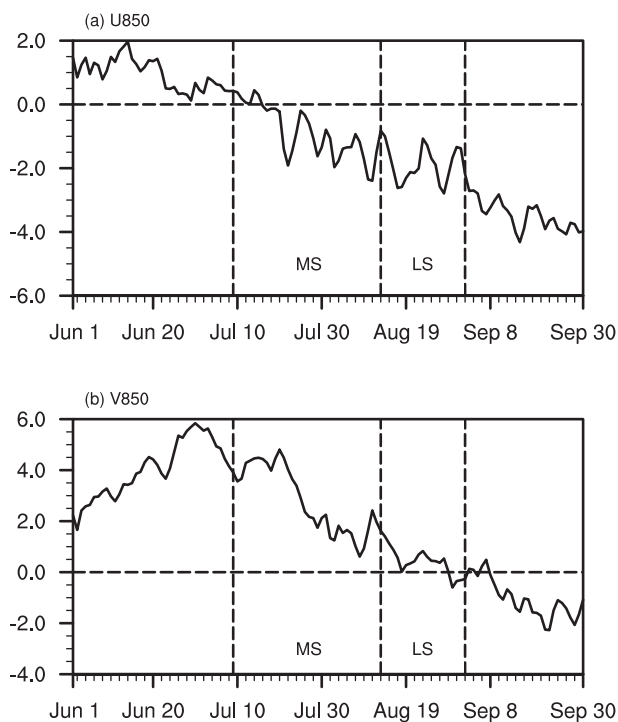


Fig. 9. Evolution of the climatological (a) zonal and (b) meridional wind (units: m s^{-1}) averaged along $(23.75^\circ\text{N}, 107.5^\circ\text{E})$, which is shown by the horizontal dashed lines in Fig. 7. The vertical dashed lines represent the periods for mid-summer and late summer.

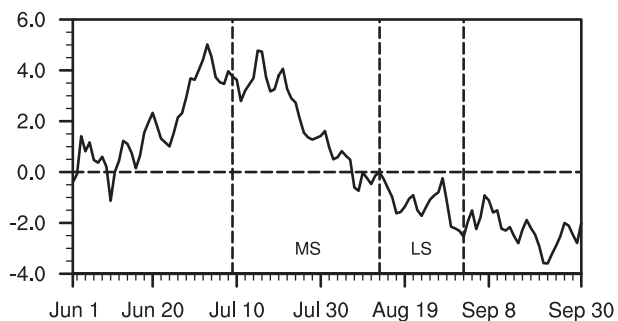


Fig. 10. Evolution of the climatological southwesterlies (units: m s^{-1}) averaged along the trace from $(22.5^\circ\text{N}, 105^\circ\text{E})$ to $(32.5^\circ\text{N}, 115^\circ\text{E})$, which is shown by the slanted dashed lines in Fig. 4. The vertical dashed lines represent the periods for mid-summer and late summer.

ing early summer and mid-summer (Li and Lu, 2018).

This study shows the rainfall anomalies over eastern China associated with the subtropical WNP anticyclonic anomaly mainly appear over CSC during late summer. The region includes the middle reaches of both the Yangtze River and Pearl River, the two largest rivers in China. Therefore, the interannual variability of the tropical WNP precipitation during late summer will play a crucial role in affecting the runoff of these two rivers, which will further exert an influence on the hydrological conditions and ecosystems of their middle and lower reaches. The lower reaches of the Yangtze River and Pearl River are the most populated areas of China, and thus a better understanding of the rainfall variability over CSC is of important significance.

Acknowledgements. We thank the two anonymous reviewers for their comments, which were helpful in improving the presentation. This work was supported by the National Natural Science Foundation of China (Grant Nos. 41721004 and 41320104007).

REFERENCES

- Chen, T.-C., S.-Y. Wang, W.-R. Huang, and M.-C. Yen, 2004: Variation of the East Asian summer monsoon rainfall. *J. Climate*, **17**(4), 744–762, [https://doi.org/10.1175/1520-0442\(2004\)017<0744:VOTEAS>2.0.CO;2](https://doi.org/10.1175/1520-0442(2004)017<0744:VOTEAS>2.0.CO;2).
- Chen, W., J.-K. Park, B. W. Dong, R. Y. Lu, and W.-S. Jung, 2012: The relationship between El Niño and the western North Pacific summer climate in a coupled GCM: Role of the transition of El Niño decaying phases. *J. Geophys. Res.*, **117**, D12111, <https://doi.org/10.1029/2011JD017385>.
- Chen, W., J.-Y. Lee, K.-J. Ha, K.-S. Yun, and R. Y. Lu, 2016: Intensification of the western North Pacific anticyclone response to the short decaying El Niño event due to greenhouse warming. *J. Climate*, **29**(10), 3607–3627, <https://doi.org/10.1175/JCLI-D-15-0195.1>.
- Chu, J.-E., S. N. Hameed, and K.-J. Ha, 2012: Nonlinear, intraseasonal phases of the East Asian summer monsoon: Extraction and analysis using self-organizing maps. *J. Climate*, **25**, 6975–6988, <https://doi.org/10.1175/JCLI-D-11-00512.1>.
- Ding, Y. H., 2005: *Advanced Synoptic Meteorology*. 2nd ed. China Meteorological Press, 585 pp. (in Chinese)
- Ding, Y. H., and J. C. L. Chan, 2005: The East Asian summer monsoon: An overview. *Meteor. Atmos. Phys.*, **89**(1–4), 117–142, <https://doi.org/10.1007/s00703-005-0125-z>.
- Han, Y. H., Z. G. Ma, Q. Yang, and Z. H. Pan, 2014: Changing characteristics of daytime and nighttime precipitation in Xinjiang under global warming. *Climatic and Environmental Research*, **19**(6), 763–772, <https://doi.org/10.3878/j.issn.1006-9585.2014.13142>. (in Chinese)
- Hu, K. M., S.-P. Xie, and G. Huang, 2017: Orographically anchored El Niño effect on summer rainfall in central China. *J. Climate*, **30**(24), 10 037–10 045, <https://doi.org/10.1175/JCLI-D-17-0312.1>.
- Huang, R. H., and F. Y. Sun, 1992: Impacts of the tropical western Pacific on the East Asian summer monsoon. *J. Meteor. Soc. Japan*, **70**(1B), 243–256, https://doi.org/10.2151/jmsj1965.70.1B_243.
- Kobayashi, S., and Coauthors, 2015: The JRA-55 reanalysis: General specifications and basic characteristics. *J. Meteor. Soc. Japan*, **93**(1), 5–48, <https://doi.org/10.2151/jmsj.2015-001>.
- Kosaka, Y., and H. Nakamura, 2010: Mechanisms of meridional teleconnection observed between a summer monsoon system and a subtropical anticyclone. Part I: The Pacific-Japan pattern. *J. Climate*, **23**(19), 5085–5108, <https://doi.org/10.1175/2010JCLI3413.1>.
- Kosaka, Y., S.-P. Xie, and H. Nakamura, 2011: Dynamics of interannual variability in summer precipitation over East Asia. *J. Climate*, **24**, 5435–5453, <https://doi.org/10.1175/2011JCLI4099.1>.
- Kurihara, K., and T. Tsuyuki, 1987: Development of the barotropic high around Japan and its association with Rossby wave-like propagations over the North Pacific: Analysis of August 1984. *J. Meteor. Soc. Japan*, **65**, 237–246, https://doi.org/10.2151/jmsj1965.65.2_237.
- Li, C. F., R. Y. Lu, and B. W. Dong, 2014: Predictability of the western North Pacific summer climate associated with different ENSO phases by ENSEMBLES multi-model seasonal forecasts. *Climate Dyn.*, **43**, 1829–1845, <https://doi.org/10.1007/s00382-013-2010-7>.
- Li, X. Y., and R. Y. Lu, 2017: Extratropical factors affecting the variability in summer precipitation over the Yangtze River basin, China. *J. Climate*, **30**(20), 8357–8374, <https://doi.org/10.1175/JCLI-D-16-0282.1>.
- Li, X. Y., and R. Y. Lu, 2018: Subseasonal change in the seesaw pattern of precipitation between the Yangtze River basin and the tropical western North Pacific during summer. *Adv. Atmos. Sci.*, **35**(10), 1231–1242, <https://doi.org/10.1007/s00376-018-7304-6>.
- Lin, Z. D., and R. Y. Lu, 2008: Abrupt northward jump of the East Asian upper-tropospheric jet stream in mid-summer. *J. Meteor. Soc. Japan*, **84**(6), 857–866, <https://doi.org/10.2151/jmsj.86.857>.
- Lin, Z. D., and R. Y. Lu, 2009: The ENSO's effect on eastern China rainfall in the following early summer. *Adv. Atmos. Sci.*, **26**(2), 333–342, <https://doi.org/10.1007/s00376-009-0333-4>.
- Lu, R. Y., 2001a: Interannual variability of the summertime North Pacific subtropical high and its relation to atmospheric convection over the warm pool. *J. Meteor. Soc. Japan*, **79**, 771–783, <https://doi.org/10.2151/jmsj.79.771>.
- Lu, R. Y., 2001b: Atmospheric circulations and sea surface temperatures related to the convection over the western Pacific warm pool on the interannual scale. *Adv. Atmos. Sci.*, **18**, 270–282, <https://doi.org/10.1007/s00376-001-0019-z>.
- Lu, R. Y., 2004: Associations among the components of the East Asian summer monsoon systems in the meridional direction. *J. Meteor. Soc. Japan*, **82**(1), 155–165, <https://doi.org/10.2151/jmsj.82.155>.
- Lu, R. Y., and B. W. Dong, 2001: Westward extension of North Pacific subtropical high in summer. *J. Meteor. Soc. Japan*, **79**(6), 1229–1241, <https://doi.org/10.2151/jmsj.79.1229>.
- Nitta, T., 1987: Convective activities in the tropical western Pacific and their impact on the Northern Hemisphere summer circulation. *J. Meteor. Soc. Japan*, **65**(3), 373–390, https://doi.org/10.2151/jmsj1965.65.3_373.
- Oh, H., and K.-J. Ha, 2015: Thermodynamic characteristics and responses to ENSO of dominant intraseasonal modes in the East Asian summer monsoon. *Climate Dyn.*, **44**(7–8), 1751–1766, <https://doi.org/10.1007/s00382-014-2268-4>.
- Qian, W. H., and D. K. Lee, 2000: Seasonal march of Asian summer monsoon. *International Journal of Climatology*, **20**(11), 1371–1386, [https://doi.org/10.1002/1097-0088\(200009\)20:11](https://doi.org/10.1002/1097-0088(200009)20:11)

- <1371::AID-JOC538>3.0.CO;2-V.
- Su, Q., R. Y. Lu, and C. F. Li, 2014: Large-scale circulation anomalies associated with interannual variation in monthly rainfall over South China from May to August. *Adv. Atmos. Sci.*, **31**(2), 273–282, <https://doi.org/10.1007/s00376-013-3051-x>.
- Su, T. H., and F. Xue, 2010: The intraseasonal variation of summer monsoon circulation and rainfall in East Asia. *Chinese Journal of Atmospheric Sciences*, **34**(3), 611–628, <https://doi.org/10.3878/j.issn.1006-9895.2010.03.13>. (in Chinese)
- Tao, S.-Y., and L. X. Chen, 1987: A review of recent research on the East Asian summer monsoon in China. *Monsoon Meteorology*, C.-P. Chang and T. N. Krishnamurti, Eds., Oxford University Press, 60–92.
- Wang, B., R. G. Wu, and X. H. Fu, 2000: Pacific–East Asian teleconnection: How does ENSO affect East Asian climate? *J. Climate*, **13**, 1517–1536, [https://doi.org/10.1175/1520-0442\(2000\)013,1517:PEATHD.2.0.CO;2](https://doi.org/10.1175/1520-0442(2000)013,1517:PEATHD.2.0.CO;2).
- Wu, R., and B. Wang, 2001: Multi-stage onset of the summer monsoon over the western North Pacific. *Climate Dyn.*, **17**, 277–289, <https://doi.org/10.1007/s003820000118>.
- Xie, P. P., and P. A. Arkin, 1997: Global precipitation: A 17-year monthly analysis based on gauge observations, satellite estimates, and numerical model outputs. *Bull. Amer. Meteor. Soc.*, **78**, 2539–2558, [https://doi.org/10.1175/1520-0477\(1997\)078<2539:GPAYMA>2.0.CO;2](https://doi.org/10.1175/1520-0477(1997)078<2539:GPAYMA>2.0.CO;2).
- Ye, H., and R. Y. Lu, 2011: Subseasonal variation in ENSO-related East Asian rainfall anomalies during summer and its role in weakening the relationship between the ENSO and summer rainfall in eastern China since the late 1970s. *J. Climate*, **24**(9), 2271–2284, <https://doi.org/10.1175/2010JCLI3747.1>.
- Zhao, P., R. H. Zhang, J. P. Liu, X. J. Zhou, and J. H. He, 2007: Onset of southwesterly wind over eastern China and associated atmospheric circulation and rainfall. *Climate Dyn.*, **28**(7–8), 797–811, <https://doi.org/10.1007/s00382-006-0212-y>.
- Zhou, T.-J., and R.-C. Yu, 2005: Atmospheric water vapor transport associated with typical anomalous summer rainfall patterns in China. *J. Geophys. Res.*, **110**, D08104, <https://doi.org/10.1029/2004JD005413>.